Implementation and Validation of a Laminar-to-Turbulent Transition Model in the Wind-US Code

Nicholas A. Denissen
Texas A&M University, College Station, Texas

Dennis A. Yoder and Nicholas J. Georgiadis
Glenn Research Center, Cleveland, Ohio

NASA STI Program . . . in Profile

Since its founding, NASA has been dedicated to the advancement of aeronautics and space science. The NASA Scientific and Technical Information (STI) program plays a key part in helping NASA maintain this important role.

The NASA STI Program operates under the auspices of the Agency Chief Information Officer. It collects, organizes, provides for archiving, and disseminates NASA's STI. The NASA STI program provides access to the NASA Aeronautics and Space Database and its public interface, the NASA Technical Reports Server, thus providing one of the largest collections of aeronautical and space science STI in the world. Results are published in both non-NASA channels and by NASA in the NASA STI Report Series, which includes the following report types:

*   TECHNICAL PUBLICATION. Reports of completed research or a major significant phase of research that present the results of NASA programs and include extensive data or theoretical analysis. Includes compilations of significant scientific and technical data and information deemed to be of continuing reference value. NASA counterpart of peer-reviewed formal professional papers but has less stringent limitations on manuscript length and extent of graphic presentations.

*   TECHNICAL MEMORANDUM. Scientific and technical findings that are preliminary or of specialized interest, e.g., quick release reports, working papers, and bibliographies that contain minimal annotation. Does not contain extensive analysis.

*   CONTRACTOR REPORT. Scientific and technical findings by NASA-sponsored contractors and grantees.

*   CONFERENCE PUBLICATION. Collected papers from scientific and technical conferences, symposia, seminars, or other meetings sponsored or cosponsored by NASA.

*   SPECIAL PUBLICATION. Scientific, technical, or historical information from NASA programs, projects, and missions, often concerned with subjects having substantial public interest.

*   TECHNICAL TRANSLATION. English-language translations of foreign scientific and technical material pertinent to NASA's mission.

Specialized services also include creating custom thesauri, building customized databases, organizing and publishing research results.

For more information about the NASA STI program, see the following:

*   Access the NASA STI program home page at *http://www.sti.nasa.gov*

*   E-mail your question via the Internet to *help@ sti.nasa.gov*

*   Fax your question to the NASA STI Help Desk at 301–621–0134

*   Telephone the NASA STI Help Desk at 301–621–0390

*   Write to:
    NASA Center for AeroSpace Information (CASI)
    7115 Standard Drive
    Hanover, MD 21076–1320

NASA

Implementation and Validation of a Laminar-to-Turbulent Transition Model in the Wind-US Code

Nicholas A. Denissen
Texas A&M University, College Station, Texas

Dennis A. Yoder and Nicholas J. Georgiadis
Glenn Research Center, Cleveland, Ohio

September 2008

Acknowledgments

Level of Review: This material has been technically reviewed by technical management.

Available from

Implementation and Validation of a Laminar-to-Turbulent Transition Model in the Wind-US Code

Nicholas A. Denissen
Texas A&M
College Station, Texas 77843

Dennis A. Yoder and Nicholas J. Georgiadis
National Aeronautics and Space Administration
Glenn Research Center
Cleveland, Ohio 44135

Abstract

A bypass transition model has been implemented in the Wind-US Reynolds Averaged Navier-Stokes (RANS) solver. The model is based on the Shear Stress Transport (SST) turbulence model and was built starting from a previous SST-based transition model. Several modifications were made to enable (1) consistent solutions regardless of flow field initialization procedure and (2) fully turbulent flow beyond the transition region. This model is intended for flows where bypass transition, in which the transition process is dominated by large freestream disturbances, is the key transition mechanism as opposed to transition dictated by modal growth. Validation of the new transition model is performed for flows ranging from incompressible to hypersonic conditions.

Nomenclature

C_f	skin friction coefficient
k	turbulent kinetic energy
M	Mach number
M_t	turbulent Mach number
P	static pressure
$\mathcal{P}_k$	production of turbulent kinetic energy
q_w	wall heat flux
R_t	turbulent Reynolds number $= \rho k / \mu \omega$
R_y	turbulent Reynolds number based on wall distance $= \rho y \sqrt{k} / \mu$
Re_x	plate Reynolds number
$Re_{\theta t}$	Reynolds number based on momentum thickness
Re_ν	vorticity-based Reynolds number
s	streamline coordinate
S_{ij}	rate of strain tensor
St	Stanton number

t	time
T_0	stagnation temperature
U_j	velocity
x, y, z	Cartesian coordinates
y^+	wall normal coordinate
κ	Von Karman constant
μ	dynamic viscosity
μ_t	dynamic eddy viscosity
ν	kinematic viscosity
ν_t	kinematic eddy viscosity
ω	specific turbulent dissipation rate
Ω	vorticity magnitude
ρ	density
τ	turbulent time scale
τ_{ij}	viscous stress tensor
τ_{ij}^T	turbulent stress tensor
∞	freestream

Introduction

This report describes the implementation of an engineering transition model in Wind-US. Wind-US is the production Reynolds Averaged Navier-Stokes (RANS) solver of the NPARC Alliance, a formal partnership of NASA Glenn Research Center and the U.S. Air Force Arnold Engineering Development Center (AEDC), with significant participation by the Boeing Company.[1] It is used by the NPARC Alliance partners and a number of other U.S. organizations spread across government, academia and industry to conduct analyses of a broad range of aerospace applications. As part of the ongoing development and improvement of the software for hypersonic simulations, as sponsored by the Office of the Secretary of Defense (OSD) Testing and Evaluation, Science and Technology (T&E/S&T) Program and the NASA Fundamental Aeronautics Program, the desire for an accurate laminar-to-turbulent transition prediction capability was highlighted.

The transition model development process began with a literature survey to select a baseline model that would fit the needs of engineers and scientists using the Wind-US solver. Once completed, a method of transition prediction was implemented and subsequently refined. After this initial code development and calibration stage, a number of experimental benchmarks were evaluated. This report describes the laminar-to-turbulent transition prediction methodology chosen and its justifications, the modifications necessary to calibrate the transition model using existing experimental data, and validation of the new model for benchmark transitional flows.

Motivation

Laminar-to-turbulent transition is a field of continuing research. Despite decades of study there are still many aspects of the transition process that are not well understood. Given this, a universally applicable and sufficiently accurate method of determining the onset of transition is not possible for most flows of common engineering interest. This is in spite of the importance of the transition onset location to the calculation of drag, heat transfer, and other boundary layer characteristics. If the transition location is not well known, substantial error can be introduced into the simulation. Therefore, it is important in engineering and design applications to be able to predict transition location to a reasonable accuracy.

The onset of transition is affected by numerous factors including the freestream flow properties such as turbulence level, Mach number, temperature, and pressure; as well as properties of the object itself such as surface temperature, surface finish, and its alignment relative to the flow. All of these factors make universal transition prediction a daunting challenge. While it is not currently possible to develop a scheme capable of taking all of these issues into account, it is possible to address specific areas and develop techniques for dealing with the instabilities caused by a more limited set of parameters.

Transition occurs due to instabilities developed in the Navier-Stokes equations that govern the physics of fluid flow. A RANS solver like Wind-US is capable of mimicking the transition process (and some such as Wilcox,[2] argue that the growth of instabilities is replicated in a somewhat similar fashion) via a rapid growth in the production of turbulence at a point in the boundary layer. However, the most commonly used RANS techniques utilize a turbulence model solving one or two additional transport equations to represent the mean turbulent effect, and universally predict the onset of transition to occur much too close to the origin of the boundary layer. That is, they generate instabilities at an unrealistically low Reynolds number, and the transition to turbulence occurs well upstream of experimental data. The motivation of the present work is to implement a method that more accurately simulates the onset of this instability, moving the numerically predicted transition location downstream to a value consistent with experimental results.

As explained above, a transition prediction scheme that is universally applicable is not currently possible. In order to narrow the scope of the problem, the present work will focus on what is known as "bypass" transition. Figure 1 shows a schematic "road map" of the transition process based on the work of Morkovin, Reshotko and Herbert.[3] On the left of the figure are the so-called natural transition mechanisms that arise from a linear stability analysis of the Navier-Stokes equations. As the magnitudes of the boundary layer disturbances increase (moving to the right side of the figure), these linear modes are "bypassed" and transition occurs more rapidly due to non-linear interactions. Freestream turbulence is one of the mechanisms that generate these disturbances. The freestream turbulence intensity (FSTI) in the levels analyzed in the present work, and typical of large high-speed wind tunnel facilities, falls into this bypass category. The focus here will be on modifying the equations solved by Wind-US to accurately reproduce the behavior of flow undergoing bypass transition due to free stream turbulence.

Bypass transition due to freestream turbulence has been studied with mixed success

for several decades. Large data sets evaluating the effect of increasing turbulence intensity on transition location have been compiled, though the agreement among them is mixed[4,5] and their applicability is somewhat limited. In addition to the shortcomings of available incompressible data, very little reliable and systematic transition data correlating onset location with disturbance environment is available for supersonic and hypersonic flows. In many instances, only general trends derived from simple correlations can be found for these complicated cases. The goal of the current model development is to serve as an engineering approximation and the present work will attempt to devise a formulation that will reproduce a transition location that falls within the spread of available data.

Turbulence Model

The Wind-US CFD code contains several turbulence models for providing closure to the RANS equations. The work described in this paper utilizes one of the most commonly used turbulence models, the Shear Stress Transport (SST) model of Menter.[6] References 7 and 8 have shown that the SST model generally provides the most accurate calculation of turbulent wall bounded flows of any of the one- or two-equation models in Wind-US. Equations 1-11 show the formulation used by Ref. 9 for the SST model with a provision for simulating transition. The model provides closure to the RANS equations through the addition of two-turbulent transport equations for the turbulent kinetic energy, k, and the specific dissipation rate, ω. This $k - \omega$ model is active near viscous wall boundaries, and away from the wall the model transitions to a formulation based on a traditional $k - \epsilon$ turbulence model. This is achieved by recasting the $k - \epsilon$ based equations into a $k - \omega$ formulation, and activating the additional terms by means of a switching function F_1.

$$\frac{\partial \rho k}{\partial t} + \frac{\partial \rho U_j k}{\partial x_j} = PTM \cdot \mathcal{P}_k - \beta^* \rho \omega k + \frac{\partial}{\partial x_j}\left((\mu + \sigma_k \mu_t)\frac{\partial k}{\partial x_j}\right) \tag{1}$$

$$\frac{\partial \rho \omega}{\partial t} + \frac{\partial \rho U_j \omega}{\partial x_j} = \frac{\alpha}{\nu_t}\mathcal{P}_k - \beta \rho \omega^2 + \frac{\partial}{\partial x_j}\left((\mu + \sigma_\omega \mu_t)\frac{\partial \omega}{\partial x_j}\right) + (1 - F_1)2\rho\sigma_{\omega 2}\frac{1}{\omega}\frac{\partial k}{\partial x_j}\frac{\partial \omega}{\partial x_j} \tag{2}$$

$$\mathcal{P}_k = \min\left[2\mu_t S_{ij}S_{ij} - \frac{2}{3}(\mu_t S_{mm} - \rho k)S_{nn} \; ; \; \mu_t \Omega^2\right] \tag{3}$$

$$F_1^* = \tanh(\text{arg}_1^4) \tag{4}$$

$$F_4 = \exp\left(-(R_y/120)^8\right) \tag{5}$$

$$F_1 = \max\left(F_1^*, F_4\right) \tag{6}$$

$$\text{arg}_1 = \min\left(\max\left(\frac{\sqrt{k}}{\beta^* \omega y}; \frac{500\nu}{\omega y^2}\right) \; ; \frac{4\rho\sigma_{\omega 2}k}{CD_{k\omega}y^2}\right) \tag{7}$$

$$CD_{k\omega} = \max\left(2\rho\sigma_{\omega 2}\frac{1}{\omega}\frac{\partial k}{\partial x_j}\frac{\partial \omega}{\partial x_j} \; ; 1.0 \times 10^{-20}\right) \tag{8}$$

and from these the turbulent viscosity is given as

$$\mu_t = \min\left(\alpha^* \frac{\rho k}{\omega} ; \frac{a_1 \rho k}{\Omega F_2}\right) \tag{9}$$

$$F_2 = \tanh(\text{arg}_2^2) \tag{10}$$

$$\text{arg}_2 = \min\left(2\frac{\sqrt{k}}{\beta^* \omega y} ; \frac{500\nu}{\omega y^2}\right) \tag{11}$$

The constants (ϕ_1) associated with these equations for the inner, $k - \omega$, model are:

$$\sigma_{k1} = 0.85, \qquad \beta_1^* = 0.09 \cdot \frac{5/18 + (R_t/8)^4}{1 + (R_t/8)^4}, \qquad \alpha_1^* = \frac{.025 + R_t/6}{1 + R_t/6},$$

$$\sigma_{\omega 1} = 0.5, \qquad \beta_1 = 0.075, \qquad\qquad\qquad \alpha_1 = \frac{5}{9} \cdot \frac{0.1 + R_t/2.7}{1 + R_t/2.7}, \qquad a_1 = 0.31$$

and the constants (ϕ_2) for the transformed $k - \epsilon$ model are:

$$\sigma_{k2} = 1.0, \qquad\qquad \beta_2^* = 0.09, \qquad\qquad \alpha_2^* = 1,$$

$$\sigma_{\omega 2} = 0.856, \qquad\qquad \beta_2 = 0.0828, \qquad\qquad \alpha_2 = 0.4403, \qquad\qquad a_1 = 0.31$$

These constants are blended using the same switching function, F_1 that is found in the model equations such that $\phi = F_1 \phi_1 + (1 - F_1)\phi_2$ for any of the given parameters.

The SST turbulence model has become popular for its ability to handle separated flows and complex geometry in the near wall region due to the strengths of the $k - \omega$ model, while maintaining the characteristics of the $k - \epsilon$ model to be more accurate in free shear layers. Also, SST has shown to be more resistant to problems resulting from non-orthogonal grids that can result from complex geometries.

The modification to these equations used to control the transition onset location is the "Production Term Modifier," PTM, found in Eq. 1 which reduces the production of turbulent kinetic energy, $\mathcal{P}_k$ in the k-equation. It is not used in the ω equation. In order to properly model fully turbulent flow, PTM must be set to 1 in the fully turbulent regions. To prevent the transition to turbulence that occurs much too far upstream in the baseline SST model, PTM should be less than 1 in the laminar boundary layer. In this way, $\mathcal{P}_k$ is limited and the transition to full turbulence occurs less rapidly. An added stipulation is that the form of PTM only use local flow quantities and not be dependent on integrated parameters such as displacement or momentum thickness. Requiring integral quantities or other non-local values requires increased computational time and risks a loss of generality for complex flows with multiple viscous walls. By relying on local terms, these problems are avoided.

The general form of PTM is taken from the model initially presented in Ref. 9 and

modified slightly in Ref. 10. Equations 12-15 show the model as described in Ref. 10.

$$PTM = 1 - 0.94(PTM1 + PTM2)F_3 \tag{12}$$

$$F_3 = e^{-\left(\frac{R_t}{5}\right)^4} \tag{13}$$

$$PTM1 = \begin{cases} 1 - [(3.28 \times 10^{-4})Re_v - (3.94 \times 10^{-7})Re_v^2 + (1.43 \times 10^{-10})Re_v^3]; & Re_v < 1000 \\ 1 - [0.12 + (1.00 \times 10^{-5})Re_v]; & Re_v > 1000 \end{cases} \tag{14}$$

$$PTM2 = \begin{cases} -|K|^{0.4}\frac{Re_v}{80}; & K < 0 \\ 0; & K > 0 \end{cases} \tag{15}$$

where the pressure gradient parameter, K, is given by

$$K = -\frac{\mu}{\rho^2 U^3}\left[1 - M^2\right]\frac{dp}{ds} \tag{16}$$

In these equations R_t is the turbulent Reynolds number and is effectively the ratio of turbulent to laminar viscosity, and $Re_v = \rho y^2 \Omega/\mu$ is the vorticity based Reynolds number. Together, the claim in Refs. 9-10 is that these terms will limit $\mathcal{P}_k$ in the laminar region where it is over-predicted by SST and allow fully turbulent production downstream.

Ref. 9 proposed a correlation in experimental data between the turbulent fluctuations upstream of transition and Re_v. It was proposed to use this correlation as a means of controlling the location of $\mathcal{P}_k$ in the wall normal direction. The quantity R_t is used to control the PTM function in the flow direction as the freestream disturbances propagate into the boundary layer. The F_3 switching function acts as a gate, determining the threshold R_t to begin turbulent production. The following sections address the performance of this initial model and the resultant changes that became necessary. In Refs. 9 and 10, $PTM2$ was formulated for flows with significant internal flow pressure gradients, and specifically for flows within low pressure turbine stages. In all cases examined in this work, where flows with significant pressure gradients were not examined, $PTM2$ was not found to be significant, and as such no modifications to this parameter are addressed in the present work.

Computational Setup

For the initial transition model investigations, all computations were performed on a zero-pressure-gradient flat plate 200 in. (5.08 m) in length. This length was selected to give the appropriate range of transitional Reynolds numbers. A region containing 21 inviscid points was used upstream of the leading edge of the plate to ensure uniform flow conditions approaching the flat plate. The number of grid points was varied considerably to investigate grid convergence and will be discussed in later sections. The computational domain was 36 in. (914.4 mm) high in the wall normal direction ending in a freestream condition. In all cases the axial points were clustered tightly in the transitional region, and the vertical points ensured a y^+ value of the first point off the wall of less than 1.

To baseline the performance of the proposed model, experimental data used by Refs. 9 and 10 was evaluated. The data used for transition in the bypass regime is given by Ref. 11 for a flat plate with a turbulence intensity at the leading edge of 3.3% referred to as the T3A data.[11] The initial simulations evaluating the proposed model duplicated these non-dimensional experimental parameters as a starting point. However, the nature of the Wind-US solver makes it very difficult to exactly duplicate the T3A conditions as the data was taken at extremely low speeds which a strictly compressible flow solver, like Wind-US, does not handle easily. However the equivalent turbulence intensity and Reynolds numbers can be matched for a case where the speed is increased to a faster, but still nearly incompressible, Mach 0.2 freestream condition.

Due to the increased freestream velocity, other parameters must be altered to give the appropriate non-dimensional conditions. To properly model the turbulence decay found in the T3A experiments, the input values of k and ω need to be specified at the inlet. These two values describe the initial turbulence intensity as well its rate of decay, and are found, for the SST model, using equations 17 and 18, where the freestream (∞) quantities are the desired dimensional values at the leading edge needed to reproduce the non-dimensional FSTI found in Eq. 19, and the values of β and β^* are those of the outer model.

$$\omega(s) = [\beta s/U_\infty + 1/\omega_\infty]^{-1} \tag{17}$$

$$k(s) = k_\infty \left[\beta \omega_\infty s/U_\infty + 1\right]^{-\beta^*/\beta} \tag{18}$$

$$\text{FSTI}(\%) = \frac{1}{U_\infty}\sqrt{\frac{2}{3}k} \tag{19}$$

Note that s is the upstream axial position relative to the leading edge, and should have a negative value. These equations are used to find the necessary upstream conditions for the simulation. It may be observed that as one moves upstream, k and ω get larger, and the dissipation rate equation (Eq. 17) in particular yields a maximum value for s that one can set an inflow upstream of the leading edge. Subsequent simulations at different FSTI levels were evaluated by changing k at the inlet. As discussed later in this report, the limiting behavior of the SST model shown in Eqs. 1 and 2 and the actual behavior of the SST model installed in Wind-US, replicate the decay of turbulence quite well.

Convergence Behavior

In the following section there will be frequent comparisons to the parameters used in the initial model. To facilitate easier comparison of the different parameters being investigated, the F_3 function defined in Eq. 13 will be referred to in the form shown in Eq. 20.

$$F_3 = e^{-\left(\frac{R_t}{\alpha}\right)^\beta} \tag{20}$$

Examining the baseline transition formulations, one finds that $\alpha = 5$ and $\beta = 4$ in the model in Ref. 10 and $\alpha = 6.5$ in the original formulation of Ref. 9. The parameters α and β used here are not to be confused with the coefficients of the baseline SST model.

The transition onset location using the method as presented by Ref. 10 demonstrates considerable sensitivity to how the solution evolves and converges in computational time. For values of $\beta > 2$ and/or $\alpha > 3$ the solution given by the transition model was found to depend strongly on whether the flow field was initialized from a converged turbulent flow, a converged laminar flow, or from uniform freestream conditions. Figure 2 shows one case where starting the solution from an initial laminar profile differed from the solution obtained by starting with an initially turbulent flow. Note that in this and subsequent figures, two correlation lines are provided on each skin friction plot, one for a fully laminar boundary layer and the other for a fully turbulent boundary layer, to compare with the transitional boundary layer solutions. These difficulties in obtaining consistent results regardless of the initialization procedure motivated efforts to modify the transition model. While Refs. 9 and 10 attempt to address this issue by suggesting the transition model only be applied after a converged laminar solution is found, generalizing the model to be independent of start-up procedure was desirable for the implementation in Wind-US discussed here.

Effect of Parameter α

An analysis of the $PTM1$ modifier in the PTM equation shows that it is relatively constant in the area of interest throughout the boundary layer in the pre-transition and transitional region, and plays a much smaller role than the F_3 switching function. Calibration of $PTM1$ will be discussed in subsequent sections.

Varying the parameter α in Eq. 20 has a large effect on both the transition location and the behavior of the solution far downstream. The physical effect of α is to serve as a threshold for activating PTM. As R_t approaches α, PTM quickly switches from laminar (no turbulent production) to a state enabling turbulent production. The transition location is dictated by where this threshold is set. In addition to the undesirable convergence behavior discussed in the previous section, the suggested value of $\alpha = 5$ from Ref. 10 not only locates the onset of transition significantly further downstream than predicted in experiments, but also causes the solution to never become fully turbulent (given this, $\alpha = 6.5$ from Ref. 9 was not evaluated). The reason for this is that very near the wall in a fully turbulent boundary layer, R_t is on the order of 5 or less into the beginning of the logarithmic region. Eq. 20 shows that the switching function for damping production, F_3, will prevent production of turbulence in the fully turbulent portion of the boundary layer, despite the fact that F_3 is only intended to be active prior to transition. Figure 3 shows the evolution of skin friction coefficient as the flow proceeds downstream. It may be observed that the skin friction coefficient for the flat-plate flow falls well short of the turbulent correlation[12] in the limit as Re_x becomes large. Reducing the value of α to 3 improves the transition onset location somewhat. However, F_3 is still damping the production of turbulence in the fully turbulent region, which results in a deficit in C_f compared to the expected value.

The cause of this can be seen quantitatively by viewing contours of the Production Term Modifier (PTM) for the two simulations. Regardless of the behavior associated with predicting the onset of transition, PTM needs to become insignificant further downstream

so as not to influence the fully turbulent region. Figures 4(a) and 4(b) show that decreasing the value of α has a marked effect on how far PTM extends into the flow, but neither value fully eliminates the downstream influence. This is problematic in that the overwhelming majority of problems of interest will have fully turbulent flow over a significant portion of the calculation domain. Even if the model were perfectly calibrated with respect to the transition location, an error in the fully turbulent behavior would still result in significant error in the downstream region. It is essential that the model produce the correct behavior far downstream for it to be a usable tool. This is a fundamental failing of the baseline model that cannot be remedied with mere "tweaks" to the calibration, and a new approach must be developed. This new approach will be detailed in the following sections.

Despite this shortcoming, and after significant numerical experimentation it was found that using a value of $\alpha = 3$ produced the most consistent results in terms of the problems associated with the flow initialization. Starting from laminar, turbulent, or uniform flow fields all produced the same result using $\alpha = 3$. This was an improvement over the baseline model formulation, and will be used as a starting point in further results.

Effect of Parameter β

To analyze the effect of β, α was held fixed at the value found in the previous section ($\alpha = 3$) and variations in β were examined. The physical effect of β is to determine how rapidly PTM changes from the laminar to turbulent production mode as one deviates from the threshold value set by α. Increasing β makes that transition more abrupt, while decreasing β leads to a more gradual change. However, as the change becomes more gradual the flow experiences the effect of PTM over a larger range of R_t, and lowering β too much produces inaccurate downstream behavior. $\beta = 2$ was found to be the most repeatable and numerically stable setting, as well as giving values in the neighborhood of the expected transition location. This result is shown in Figure 5. Although in this instance $\beta = 2$ and $\beta = 4$ are in agreement, this is not universally the case. $\beta = 2$ was used as a starting point for future work to make the transition process more gradual.

Effect of Grid Resolution

In order to study the effect of grid resolution, the optimized combination of α and β was chosen ($\alpha = 3$, $\beta = 2$). Grids were created with two different numbers of points in the wall normal direction ($j = 161$ and 321) and a progressively increasing number of points in the stream-wise direction ($i = 230$ through $i = 1023$). The present model was found to be quite sensitive to axial grid resolution, for reasons that are as yet unknown. Work by Rumsey[13] documents similar sensitivity, and an evaluation of the unmodified SST model shows that its (much too early) transition location, in fully turbulent mode, is also strongly dependent on grid spacing although it is typically ignored. It should be noted that this is not a particular deficiency of the SST model as all two-equation models seem to demonstrate this behavior in

fully turbulent mode. Figure 6 shows the resolution needed to achieve grid independence. In the present work, over 700 axial points were found to be necessary for the baseline conditions of 3.5% FSTI and Mach 0.2. Only two values of wall normal spacing were evaluated as they produced consistent results. More specifically, the region well beyond the transition location ($Re_x \geq 10^6$) contained only 50 points, meaning over 650 points were required in the first initial part of the flat plate in order to achieve a grid independent answer. The points in the transition region were clustered such that $\Delta x^+ = 62.8$ calculated using a nominal $C_f = 0.003$.

For an engineering tool the grids required to obtain solutions independent of resolution and the associated computational time necessary are somewhat prohibitive. This sensitivity of transition location was observed by others (i.e. Ref. 13). In Ref. 14, the streamwise grid sensitivity was attributed to the first oder upwinding of the advection terms in the turbulence model. Our attempts to use higher order upwinding and TVD schemes were unsuccessful in reducing the grid sensitivity. The single biggest hurdle that remains in the use of this model will continue to be the density of the grid needed to accurately resolve the transition location. The results in the following sections should be viewed in context of this shortcoming.

F_3 Correction

The preceding sections establish a baseline model that already exhibits substantial improvements over the initial form of Ref. 10. Specifically, it converges to a consistent solution regardless of initial values, and the transition onset is more consistent with experimental data. Once this base was established, further numerical experimentation was undertaken to improve overall accuracy and generality of the model. The sensitivity to grid spacing, current transition location, and the general shape of the transition region all pointed to the fact that a more gradual switching function, F_3, for controlling PTM was necessary. However, this switching needs to be done without altering the correct limiting behavior already found for the F_3 function. That is, F_3 should remain the same as $R_t \to 0$ and as $R_t \to \infty$, but smooth the transition in between. In addition, the function should not remove the production of turbulence near the wall in the fully turbulent region. Two corrections to the form of F_3 to accomplish this are described in the subsequent sections.

To moderate the behavior of F_3 in the transition region while maintaining its behavior at the extremes, the pass band of a Gauss filter was used to expand the values of R_t that kept F_3 in an area of 50% production, while the stop band prevented any changes as $R_t \to 0$ and as $R_t \to \infty$. The distribution was centered around α and expanded to produce the proper transition location. Table 1 shows the comparison between the initial model and the final value of F_3 that was found after numerical experimentation. This result is displayed graphically in Figure 7. The more gradual change in F_3 serves to decrease sensitivity and also to locate the transition onset properly.

Questions may be raised regarding the deviation of the new F_3 modifier from the initial formulations. There is no reason to expect the shape to have any unforeseen effects on the

Initial	Current
$F_3 = e^{-(R_t/5)^4}$	$F_3 = e^{-\left(\frac{R_t}{3}\right)^2}(1 - P(R_t)) + \frac{1}{2}P(R_t)$
	$P(R_t) = \frac{2.5}{\sqrt{2\pi}}e^{\frac{-(R_t-3)^2}{2}}$

Table 1: F_3 Comparison

behavior of solution despite this. Recall that the role of F_3 is to act as a gate, allowing the generation of turbulence above some threshold value of R_t. The present functional form of F_3 simply increases the range over which moderate but not full production is taking place. Maintaining the exponential decay at the extremes prevents the function from introducing undesirable behavior.

Fully Turbulent Correction

The change in the prior section to the F_3 switching function is designed to remedy problems with the profile and transition location, but the downstream behavior in the fully turbulent region remains an issue. To prevent PTM from continuing to act in the downstream region, a limiter based on the non-dimensional coordinate y^+ is employed.

$$y^+ = \frac{y\sqrt{\frac{\tau_w}{\rho_w}}}{\mu/\rho} \tag{21}$$

The parameter y^+ was chosen because it has predictable behavior relative to the turbulent boundary layer and is calculated on a point-wise basis, (i.e. it does not require any integral quantities to be calculated). The proposed downstream limiter is given by the form shown in Eq. 22 and was calibrated to eliminate the downstream remnants of PTM which are necessary in the laminar and transition regions but needs to be eliminated for the fully turbulent region.

$$F_{3(modified)} = F_3 \tanh\left((y^+/17)^2\right) \tag{22}$$

Figure 8 shows the correction's effectiveness in eliminating unwanted downstream behavior and allowing fully turbulent production. In these plots, the sharp decline in the contours indicates the transition location. Equation 22 introduces an additional dependence to the PTM formulation, which is now a function of R_t, Re_v and y^+.

One concern in using this form of limiter was that the formulation would not limit turbulent production in the laminar region near the wall where it might be necessary. However, evaluation of the flow field indicated that $\mathcal{P}_k$ is insignificant in this region when the flow is laminar (due to low strain rate/vorticity, see Eq. 3) and thus was found to have no negative effects in the upstream laminar region. Downstream, it enables fully turbulent production and allows the skin friction profiles to accurately approach values specified in various correlations. While relying on y^+ as a limiter deviates from the philosophy of the Menter SST turbulence model (and underlying Wilcox $k - \omega$ near wall model), the formulation enables the correct fully turbulent behavior and justifies its use here.

$PTM1$ and Experimental Validation-Incompressible

Given the extent to which the original model of Ref. 10 has been changed, the original formulation for $PTM1$ was examined following the reformulation of F_3. The new modifier should still be based on Re_v to exploit the properties outlined in Ref. 9 and properly account for freestream turbulence intensity. Specifically, a correlation between fluctuation intensity and Re_v is selected to correctly locate $\mathcal{P}_k$ in the boundary layer. The modified expression that was investigated is as follows:

$$PTM1 = 1 - C_{PTM1} \begin{cases} [(3.28 \times 10^{-4})Re_v - (3.94 \times 10^{-7})Re_v^2 + (1.43 \times 10^{-10})Re_v^3]; & Re_v < 1000 \\ [0.12 + (1.00 \times 10^{-5}Re_v]; & Re_v > 1000 \end{cases}$$

(23)

where $C_{PTM1} = 1.0$ to yield the baseline formulation and the effect of increasing C_{PTM1} was investigated as discussed next.

To examine variation in C_{PTM1}, we return to the T3A case described in previous sections. Unlike the simulations used for the benchmarks, where the T3A conditions served as an approximate starting point, the present simulation is matched to the precise turbulence intensity (3.3% at the leading edge) and decay rate as the experimental data. The SST model does a good job of reproducing the FSTI decay found in the T3A wind tunnel as the flow progresses downstream. Figure 9 shows a comparison between the decay found in Ref. 11 and the decay in the simulation. Despite the fairly steep gradients found here, the decay rate and initial value are successfully reproduced. Note that this plot shows a slight undershoot on the freestream intensity, which leads to an expectation that the transition onset in the simulation will occur slightly downstream of where it occurs in the experiment.

Figure 10 shows a comparison of C_f for simulations of the T3A flat plate with and without the transition model. The fully turbulent SST solution shows the more rapid transition (much closer to a fully turbulent flow) that provided the impetus for the present work. It does a poor job of accurately capturing the early laminar behavior and the transition location which would lead to incorrect results for the drag on this flat plate. For the transition model solutions, the effect of C_{PTM1} is to control the transition onset location. As with nearly all RANS-based transition prediction schemes, the width of the calculated transition region is shorter than indicated by experimental data. The solution with $C_{PTM1} = 2.0$ captures the transition onset location best while decreasing C_{PTM1} to 1.0 (default value from original formulation) captures the end of the transition zone (i.e. where fully turbulent flow is realized) best.

Figure 11 shows the results of simulations for the T3A test case where several freestream intensities are investigated using $C_{PTM1} = 1.0$ and $C_{PTM1} = 2.0$, the bounds on the recommended values of C_{PTM1}. In this figure, the ordinate is the transition Reynolds number based on θ, the momentum thickness. The plot is presented in this manner because the most frequently used engineering correlations are calibrated based on this method. In Fig. 11 the transition onset location is defined as the minimum C_f, and the FSTI is defined midway

between the leading edge and the transition location to keep in convention with how the correlations were formulated.[4,5] This method of reporting the FSTI is an attempt to account for the decay of the turbulence in the tunnel in a simple and useful way. To maintain consistency, the numerical results are also plotted in this way. The results shown in Fig. 11 indicate that the $C_{PTM1} = 2.0$ solutions match the onset of transition location somewhat better that $C_{PTM1} = 1.0$. Recall that the results of Fig. 10 showed that $C_{PTM1} = 1.0$ matches the end of transition region (fully turbulent) location better.

The range of applicability demonstrated here makes the model appropriate within the regime of "bypass" transition flow situations introduced earlier. While the model will likely have difficulty handling freestream intensities that approach zero, as well as very high disturbance environments, it should perform well in predictions for a range of conventional wind tunnels. One comment about the freestream intensity is necessary here. The correlations used as experimental validation for the model are based upon grid-generated turbulence. At a point in the wind tunnel upstream of the leading edge of the plate a disturbance generator is placed in the flow to create isotropic turbulence whose magnitude can be properly controlled. Because these are disturbances placed into an otherwise "quiet" wind-tunnel, the FSTI decays in the stream-wise direction. In contrast, turbulence found in conventional wind-tunnels comes from a variety of sources including acoustics and inflow irregularities which may not decay as the flow proceeds down the tunnel. While the transition model itself would likely have little problem handling a constant FSTI as opposed to the decaying FSTI values used in the current simulations, the limiting form of the model has difficulty replicating this constant-turbulence behavior. More work is necessary to address the FSTI decay rate in the tunnels being simulated, and if this value is a constant, additional terms may be necessary in the turbulence model to generate this disturbance at an appropriate level.

In concluding this section, we summarize the final form of the transition model that is recommended based on the modifications discussed in this report:

$$PTM = 1 - 0.94(PTM1 + PTM2)\, F_3 \tanh\left((y^+/17)^2\right) \tag{24}$$

$$F_3 = e^{-\left(\frac{R_t}{3}\right)^2}(1 - P(R_t)) + \frac{1}{2}P(R_t) \tag{25}$$

$$P(R_t) = \frac{2.5}{\sqrt{2\pi}}e^{\frac{-(R_t-3)^2}{2}} \tag{26}$$

$$PTM1 = 1 - C_{PTM1}\begin{cases} [(3.28E-4)Re_v - (3.94E-7)Re_v^2 + (1.43E-10)Re_v^3]; & Re_v < 1000 \\ [0.12 + (1E-5)Re_v]; & Re_v > 1000 \end{cases} \tag{27}$$

$$1.0 \le C_{PTM1} \le 2.0 \qquad (Recommended \quad range) \tag{28}$$

In Wind-US, the default value for C_{PTM1} is set to 1.

Experimental Validation-Compressible

Experimental data systematically analyzing the effect of freestream turbulence in higher Mach number flows is not as prevalent as in the incompressible case. Concrete correlations for higher Mach numbers equivalent to those used in the incompressible cases are not readily available. The most frequently used tools in current use involve single point correlations of the form $Re_\theta/M = $ constant. These correlations have been developed in free flight conditions and in conventional supersonic tunnels and can be used to establish trends regarding the transition behavior at varying Mach numbers. The accuracy of these correlations is uncertain and comparing the model to them in any quantitative way is difficult, but qualitative comparisons are useful and are examined here.

A series of cases was examined for Mach 2.5, 3.5, and 4.5 to investigate the performance of the transition model in supersonic flow. A computational grid having 661 axial points and 161 points in the wall normal direction was used. These supersonic cases demonstrated lower grid sensitivity than for the incompressible cases in that solutions obtained with every other grid point in each direction were very similar to those using the full grid. Since we are interested in comparing locations of transition onset, the simulations used $C_{PTM1} = 2.0$. Figure 12 shows a plot similar to that used for the incompressible calibration, with the lines of $Re_\theta/M = 100$ plotted for the Mach numbers being simulated.[15] The shaded region shows the same expected transition band from the incompressible correlations of Fig. 11 only for reference. The results for these supersonic cases show that in the range of turbulence intensities common in supersonic wind-tunnels, the model is able to qualitatively reproduce the experimentally determined behavior. The parameters for the numerical simulation are the same as in the previous section, changing only the Mach number and initial turbulent intensity. The model is able to successfully reproduce the known stabilizing influence of higher Mach number flows.

While none of the numerical data points correspond precisely to the correlations shown in Fig. 12, it has been documented that the model varies smoothly with increasing and decreasing intensities. It would not be difficult, nor would it be any more revealing, to find the exact FSTI that reproduces the transition location found with these simple correlations. In addition, this method of correlating the transition location has been under scrutiny.[16] These correlations are used here merely to establish a general trend and the relative magnitude of the expected changes due to compressibility effects. The lack of other meaningful empirical comparisons makes more sophisticated analysis difficult.

Experimental Validation-Hypersonic

Hypersonic flows present unique challenges in both modeling and experimentation. To baseline the present model's ability to predict transitional behavior in hypersonic conditions, it was validated against transition data taken in the AEDC tunnel B on sharp nose cones at Mach 7.93.[17] The simulation is performed on a 7° half angle cone, 40 inches (1016.3 mm) in length, in agreement with Ref. 17, and as in the experiment, the wall temperature was set at

$0.42T_0$, where T_0 is the freestream stagnation temperature. Several unit Reynolds numbers (Re/m) were evaluated in Ref. 17 to provide a complete scan of the transition region. These data show good agreement across a range of Re/m, allowing the simulation to use only one, $\approx 6.8 \times 10^6$ Re/m, corresponding closely with the center of the experimental range. As in previous cases, the grid was clustered near the transition location and used 338 axial points and 161 points in the wall normal direction, maintaining a y^+ of the first point off the wall less than 1. Inflow conditions are calculated to match those of Ref. 17 and insight by Ref. 18 that an inlet FSTI of 1.25% was appropriate for AEDC tunnel B.

Figure 13 shows static pressure contours to validate the development of the shock around the cone. The shock angle is in very close agreement with theoretical predictions and demonstrates there is no need for further grid refinement to accurately capture the shock behavior. Figure 14 shows the Stanton number (St) as defined by Ref. 17 (and as shown in Eq. 29) versus Reynolds number for the SST model alone, the SST transition model using $C_{PTM1} = 1.0$ and $C_{PTM1} = 2.0$, and the experimental data.

$$St = \dot{q_w}/(\rho_\infty U_\infty (h(T_0) - h(T_w))) \tag{29}$$

Although as in the incompressible case the behavior in the transition region itself is overly abrupt, the model accurately captures the minimum heat transfer value, corresponding to transition onset for $C_{PTM1} = 2.0$ and the location where the follow becomes fully turbulent for $C_{PTM1} = 1.0$.

Of additional interest is the agreement of the simulation with the pre-transition data. The SST transition model accurately captures the laminar heat transfer behavior in the region leading up to transition. This is important in demonstrating the utility of the model, as finding a correct transition location would be irrelevant if the model was unable to produce the accurate laminar behavior prior to onset. Additionally, this is a non-trivial validation as the y^+ limiter placed in the PTM function allows for some turbulent production in the near wall region, even when the flow is laminar. However, the agreement between the transition model and the data verifies that this modifier has no noticeable effect on the flow behavior in the laminar region, even in the hypersonic case. Although no specific experimental case is shown for supersonic validation, the ability of the model to match behavior at subsonic and hypersonic Mach numbers demonstrates consistency across different flow regimes.

This is a marked improvement over the SST model alone, which vastly over-predicts the heat transfer by indicating a fully turbulent state from the leading edge of the test article. For a model in a high-speed wind-tunnel that has a significant laminar region, the error due to transition onset can be quite large. The total heat transfer integrated over the length of the cone differs by 38.7% between the SST model and the transitional SST model with $C_{PTM1} = 1.0$. Accurately capturing this behavior is especially important when trying to evaluate thermal properties and heat transfer behavior near the tip of a hypersonic vehicle. The large discrepancy in heat transfer rates indicated by the two models would substantially alter the vehicle's predicted temperature profile.

Conclusions

A laminar-to-turbulent transition method has been implemented and validated in the Wind-US flow solver. This method was built starting from a previous formulation centered around the Menter SST turbulence model, with significant modifications enabling a more accurate engineering calculation tool. The transition prediction model in the present work demonstrates several improvements over the previous form presented in Ref. 10. The current form of the "Production Term Modifier" prevents problematic convergence behavior, allows fully turbulent production downstream of the transition location, and is found to reproduce transition onset accurately in a wide range of zero or slight pressure gradient flows. The model is intended for flows where bypass transition is the dominant laminar-to-turbulent transition mechanism, and is validated against experimental data for cases ranging from incompressible to hypersonic over a range of inlet turbulence intensities. While the model remains overly grid sensitive, and does not exactly replicate the behavior in the transitional region between fully laminar and fully turbulent, it nevertheless constitutes an improved engineering tool for finding behavior in flows where transitional effects are significant. Further, it accomplishes this without the expense of adding any additional transport equations or requiring calculation of integrated parameters such as momentum thickness. This allows the model to be more efficient and avoid the ambiguities inherent when integrating in the wall normal direction with complex geometries.

This report serves as a starting point for incorporating more accurate transition prediction into the Wind-US solver. More work into models involving additional transport equations, pressure gradients, and natural transition effects is necessary to cover the broad scope of transition phenomena. Additionally, efforts to eliminate the grid sensitivity that remains in the present model should be explored. Despite these limitations, this transition model represents an improvement in the ability of computational methods to complement wind-tunnel testing at a range of Mach numbers.

References

[1] Nelson, C. C. and Power, G. D., "CHSSI Project CFD-7: The NPARC Alliance Flow Simulation System," *39th AIAA Aerospace Sciences Meeting and Exhibit - AIAA-2001-0594*, January 2001.

[2] Wilcox, D. C., "Simulation of Transition with a Two-Equation Turbulence Model," *AIAA Journal*, Vol. 32, No. 2, February 1994, pp. 247–255.

[3] Morkovin, M. V., Reshotko, E., and Herbert, T., "Transition in Open Flow Systems - A Reassessment," *Bull. APS*, Vol. 39, No. 9, 1994, pp. 1–31.

[4] Mayle, R. E., "The Role of Laminar-Turbulent Transition in Gas Turbine Engines," *ASME Journal of Turbomachinery*, Vol. 113, 1991, pp. 509–537.

[5] Abu-Ghannam, B. J. and Shaw, R., "Natural Transition of Boundary Layers - The Effects of Turbulence, Pressure Gradient, and Flow History," *Journal of Mechanical Engineering Science*, Vol. 22, No. 5, October 1980, pp. 213–228.

[6] Menter, F. R., "Zonal Two Equation $k-\omega$ Turbulence Models for Aerodynamic Flows," *24th AIAA Fluid Dynamics Conference - AIAA-93-2906*, July 1993.

[7] Dippold III, V., "Investigation of Wall Function and Turbulence Model Performance within the Wind Code," *43rd AIAA Aerospace Sciences Meeting and Exhibit - AIAA-2005-1002*, January 2005.

[8] DalBello, T., Georgiadis, N. J., Yoder, D. A., and Keith, T. G., "Computational Study of Axisymmetric Off-Design Nozzle Flows," *42nd AIAA Aerospace Sciences Meeting and Exhibit - AIAA-2004-0530*, January 2004.

[9] Langtry, R. B. and Sjolander, S. A., "Prediction of Transition for Attached and Separated Shear Layers in Turbomachinery," *AIAA/ASME/SAE/ASEE Joint Propulsion Conference and Exhibit - AIAA-2002-3641*, July 2002.

[10] Menter, F., Ferreira, J. C., Esch, T., and Konno, B., "The SST Turbulence Model with Improved Wall Treatment for Heat Transfer Predictions in Gas Turbines," *Proceedings of the International Gas Turbine Congress - IGTC2003-TS-059*, November 2003.

[11] Savill, A. M., "Some Recent Progress in the Turbulence Modeling of Bypass Transition," *Near-Wall Turbulent Flows*, edited by C. S. R.M.C. So and B. Launder, 1993, pp. 829–848.

[12] Schlichting, H., *Boundary-Layer Theory*, McGraw-Hill, 1979.

[13] Rumsey, C. L., Thacker, W. D., Gatski, T. B., and Grosch, C. E., "Analysis of Transition-Sensitized Turbulent Transport Equations," *39th AIAA Aerospace Sciences Meeting and Exhibit - AIAA-2005-0523*, January 2005.

17

[14] Langtry, R., *A Correlation-Based Transition Model using Local Variables for Unstructured Parallelized CFD Codes*, Ph.D. thesis, University of Stuttgart, 2006.

[15] Anderson, J. D., *Hypersonic and High Temperature Gas Dynamics*, McGraw-Hill, 1989.

[16] Reshotko, E., "Is Re_θ/M a Meaningful Transition Criteria?" *AIAA Journal*, Vol. 45, No. 7, July 2007, pp. 1441–1443.

[17] Kimmel, R. L., "The Effect of Pressure Gradients on Transition Zone Length in Hypersonic Boundary Layers," *Journal of Fluids Engineering*, Vol. 119, March 1997, pp. 36–41.

[18] McDaniel, R. D. and Hassan, H. A., "Role of Bypass Transition in Conventional Hypersonic Facilities," *39th AIAA Aerospace Sciences Meeting and Exhibit - AIAA-2001-0209*, January 2001.

1 Figures
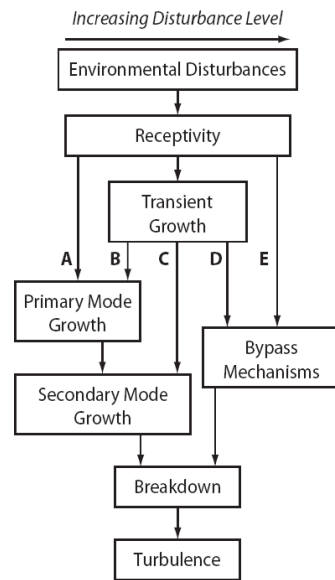
Figure 1: Transition road map, from Ref. 3
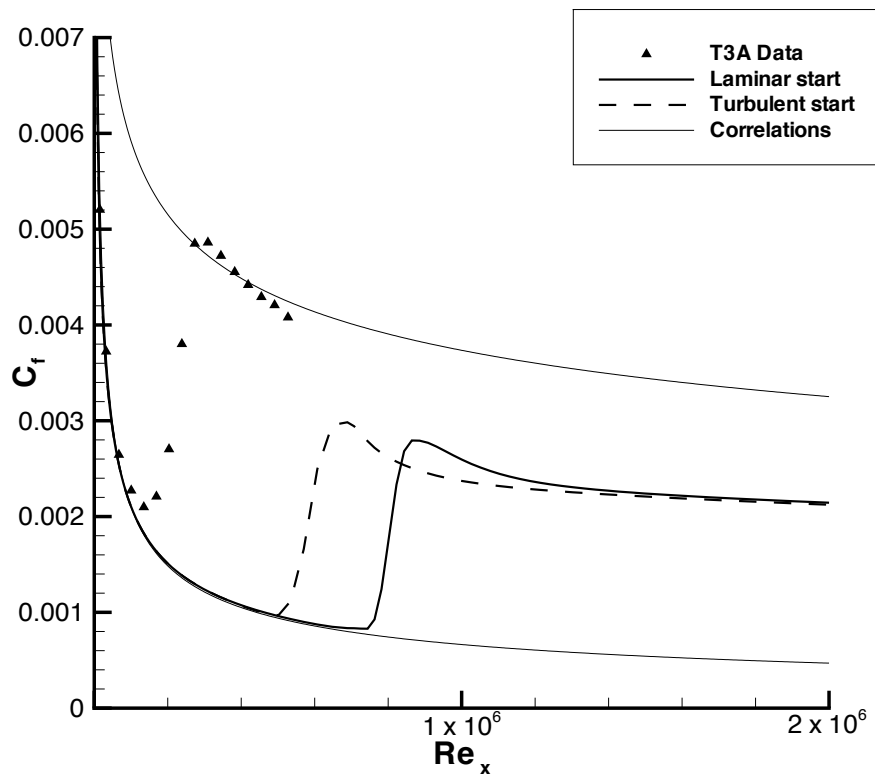
Figure 2: Spurious solutions demonstrating initialization effect
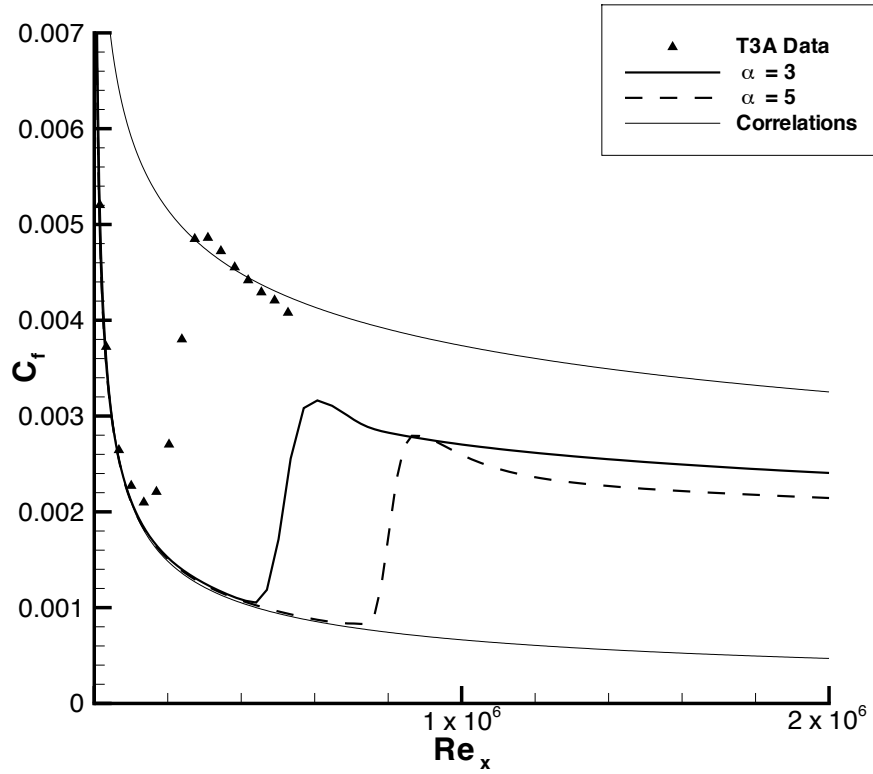
Figure 3: Dependence of transition onset on α

(a) $\alpha = 5$
(b) $\alpha = 3$
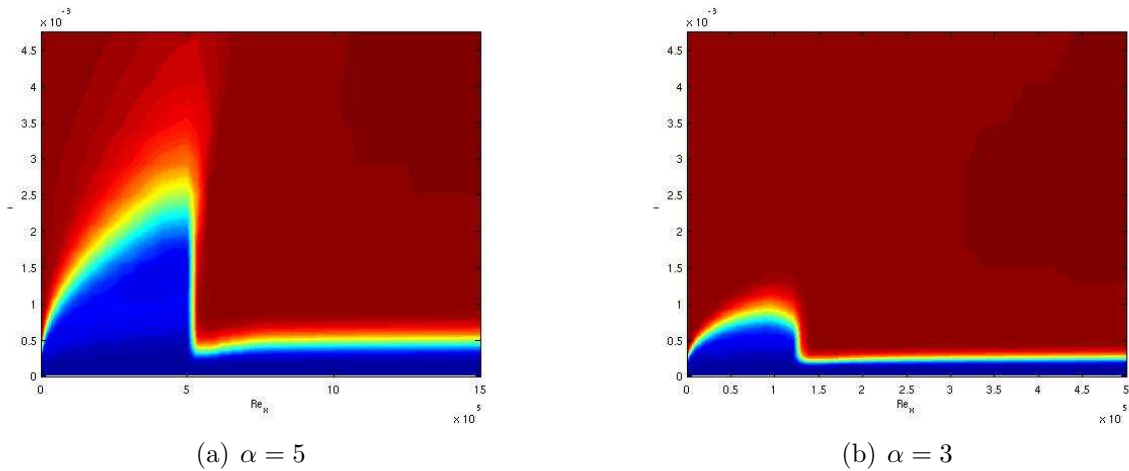
Figure 4: *PTM* Contours
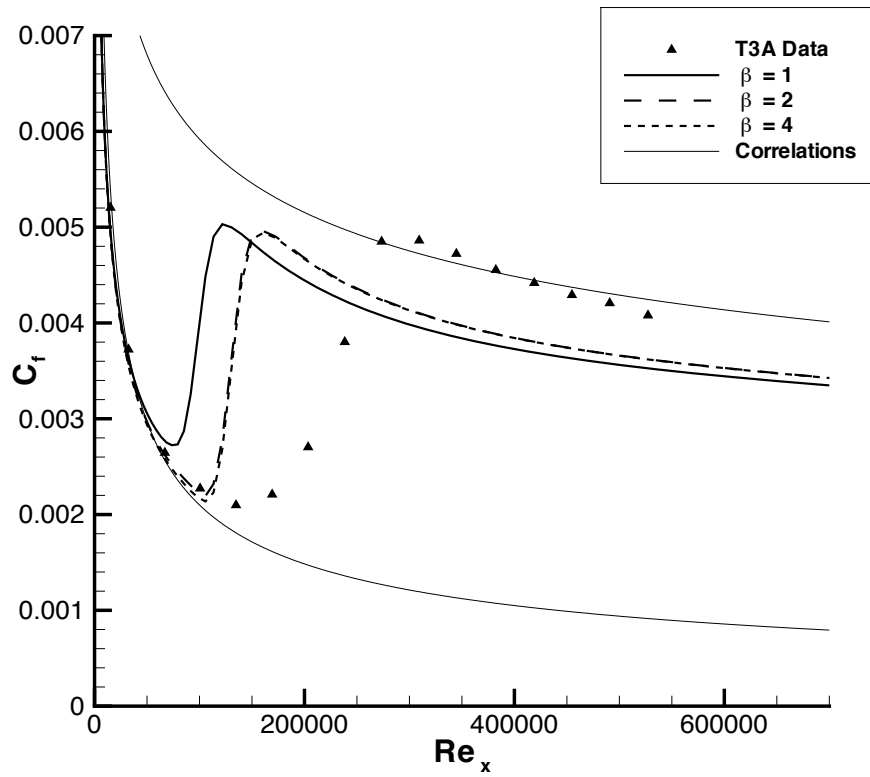
Figure 5: Dependence of transition onset on β
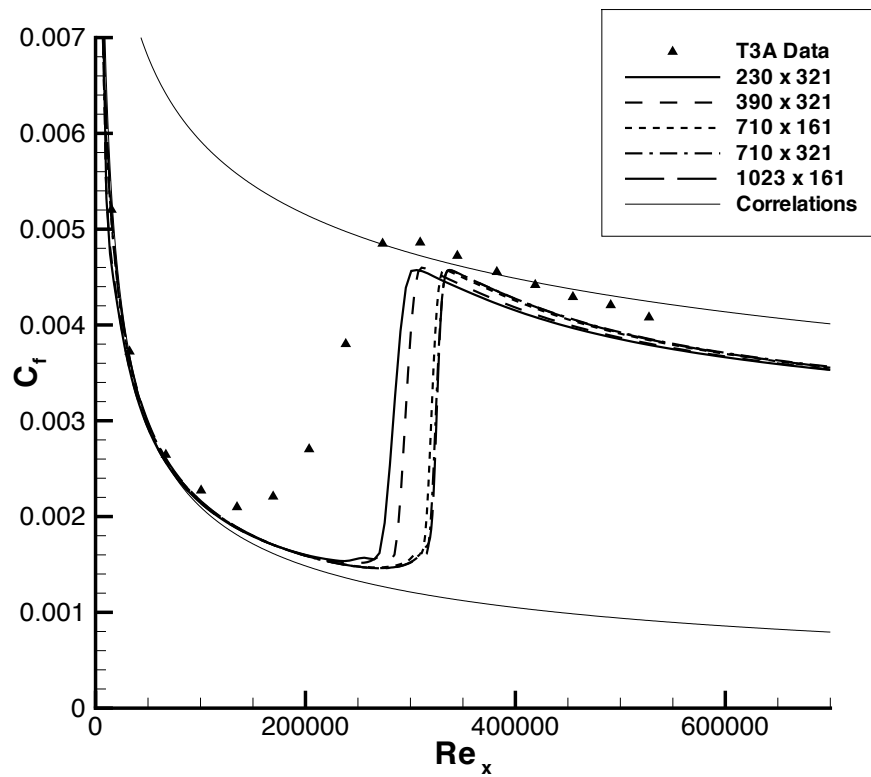
Figure 6: Grid convergence
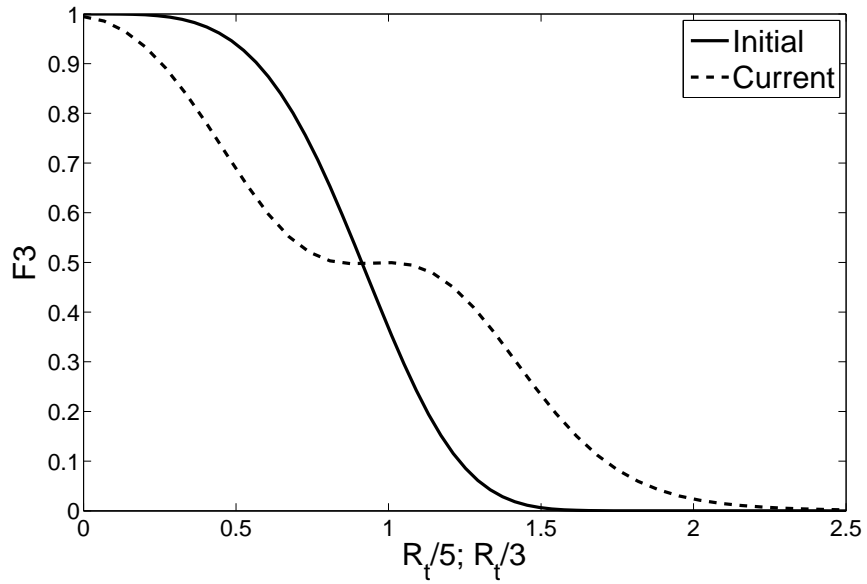
Figure 7: Comparison of original and modified F_3 functional forms

(a) F3 Contours without y^+ limiter

(b) F3 Contours with y^+ limiter
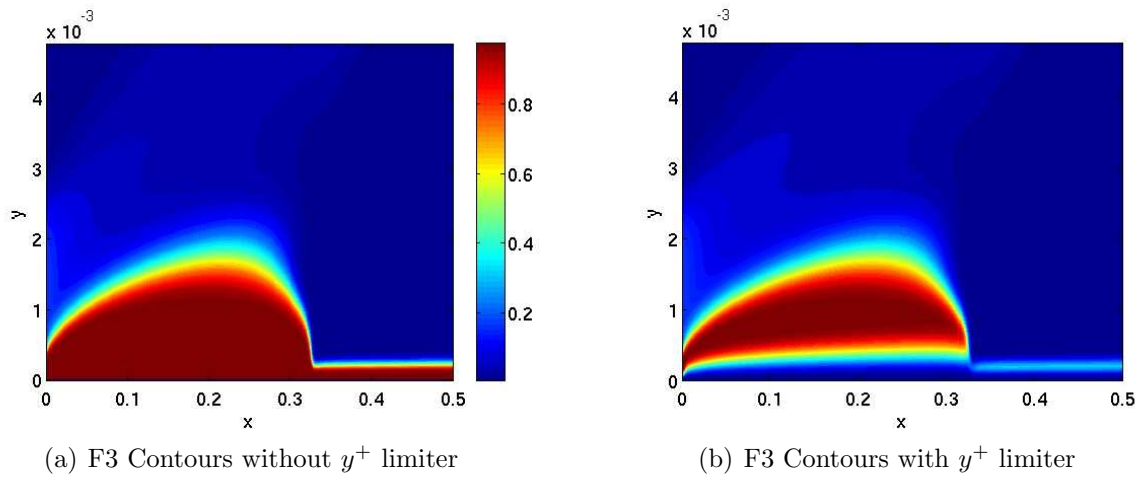
Figure 8: Comparison of F_3 contours with and without $y+$ limiter
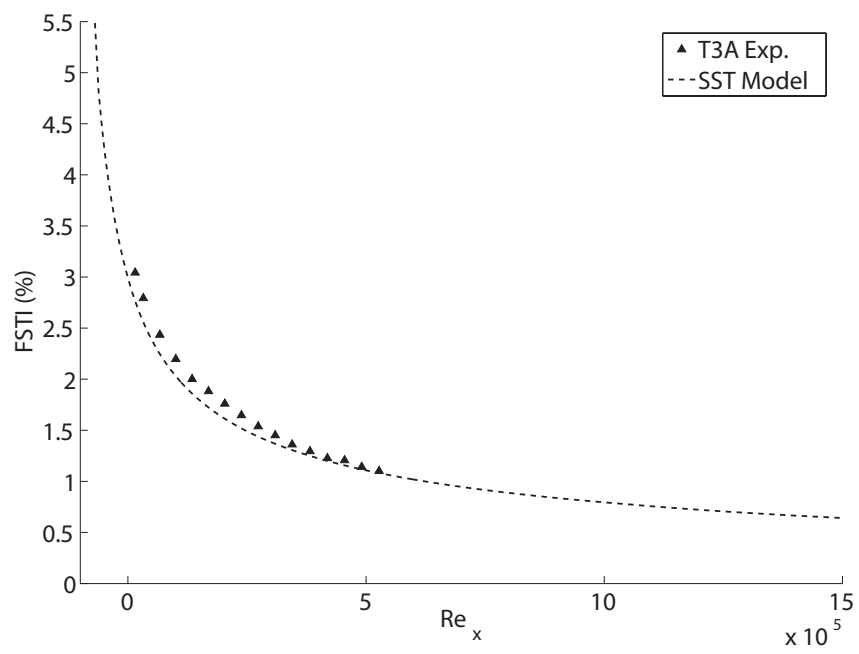
Figure 9: FSTI comparison
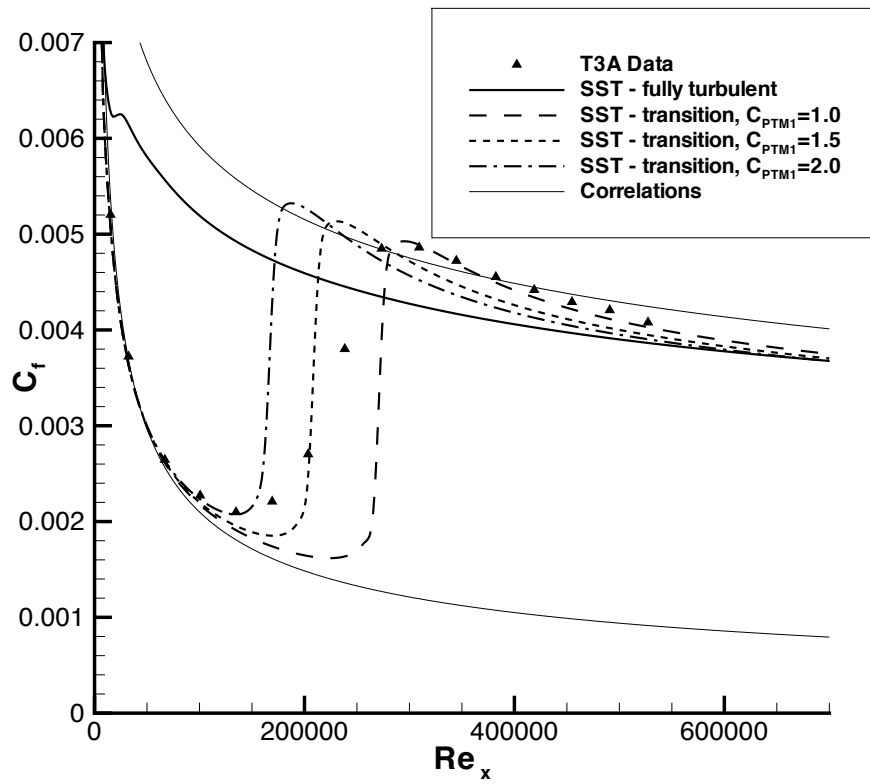
Figure 10: Transition comparison
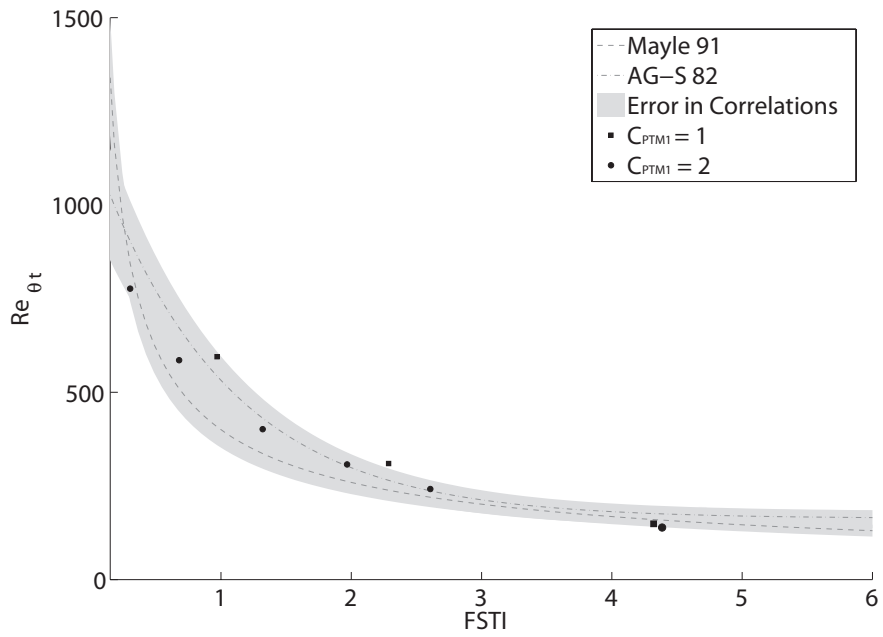
Figure 11: $PTM1$ Calibration
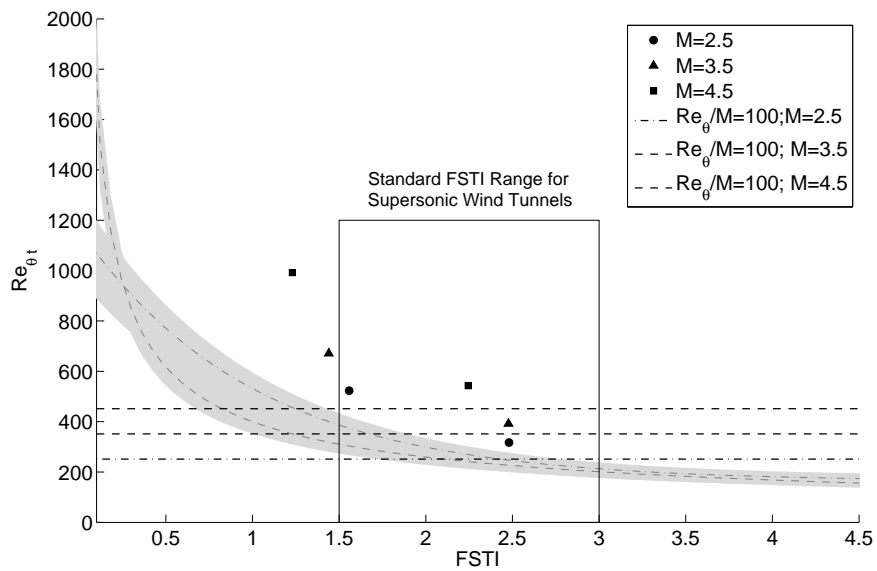
Figure 12: Supersonic Mach number comparison
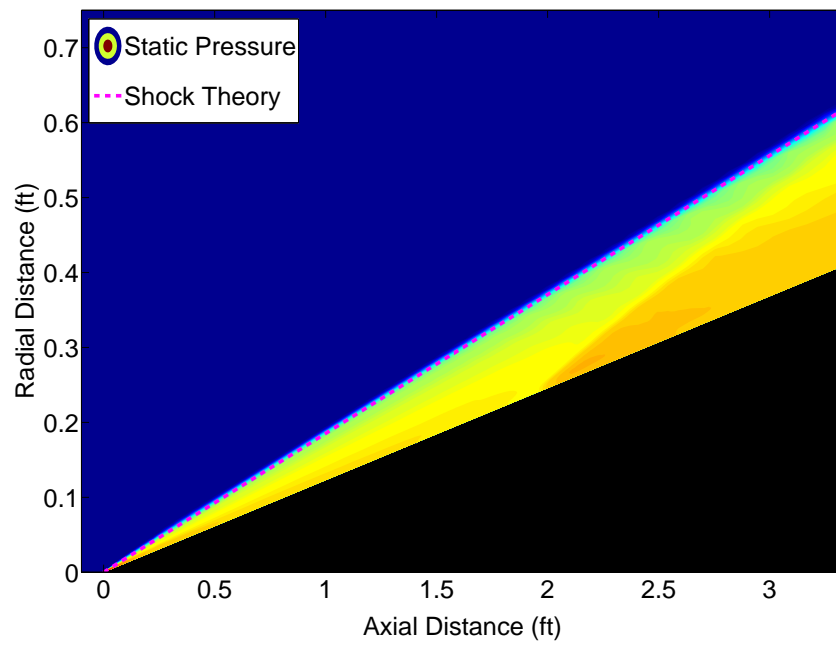
Figure 13: Hypersonic cone shock
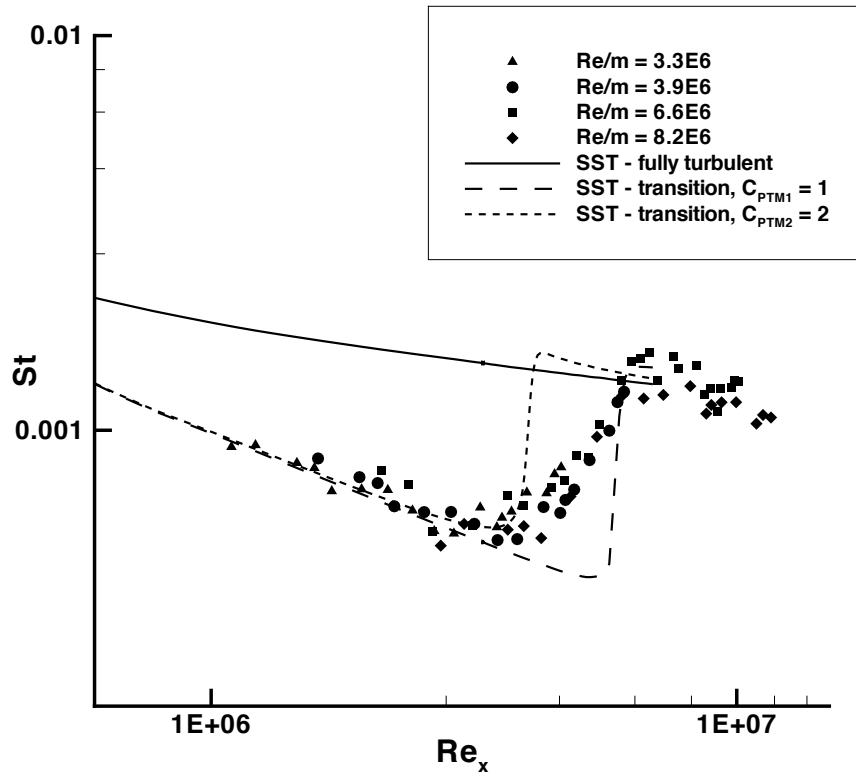
Figure 14: Hypersonic comparison

1. REPORT DATE *(DD-MM-YYYY)* 01-09-2008	2. REPORT TYPE Technical Memorandum	3. DATES COVERED *(From - To)*

4. TITLE AND SUBTITLE Implementation and Validation of a Laminar-to-Turbulent Transition Model in the Wind-US Code	5a. CONTRACT NUMBER
	5b. GRANT NUMBER
	5c. PROGRAM ELEMENT NUMBER
6. AUTHOR(S) Denissen, Nicholas, A.; Yoder, Dennis, A.; Georgiadis, Nicholas, J.	5d. PROJECT NUMBER
	5e. TASK NUMBER
	5f. WORK UNIT NUMBER WBS 599489.02.07.03.03.02.01

7. PERFORMING ORGANIZATION NAME(S) AND ADDRESS(ES) National Aeronautics and Space Administration John H. Glenn Research Center at Lewis Field Cleveland, Ohio 44135-3191	8. PERFORMING ORGANIZATION REPORT NUMBER E-16671

9. SPONSORING/MONITORING AGENCY NAME(S) AND ADDRESS(ES) National Aeronautics and Space Administration Washington, DC 20546-0001	10. SPONSORING/MONITORS ACRONYM(S) NASA
	11. SPONSORING/MONITORING REPORT NUMBER NASA/TM-2008-215451

12. DISTRIBUTION/AVAILABILITY STATEMENT
Unclassified-Unlimited
Subject Category: 02
Available electronically at http://gltrs.grc.nasa.gov
This publication is available from the NASA Center for AeroSpace Information, 301-621-0390

13. SUPPLEMENTARY NOTES

14. ABSTRACT
A bypass transition model has been implemented in the Wind-US Reynolds Averaged Navier-Stokes (RANS) solver. The model is based on the Shear Stress Transport (SST) turbulence model and was built starting from a previous SST-based transition model. Several modifications were made to enable (1) consistent solutions regardless of flow field initialization procedure and (2) fully turbulent flow beyond the transition region. This model is intended for flows where bypass transition, in which the transition process is dominated by large freestream disturbances, is the key transition mechanism as opposed to transition dictated by modal growth. Validation of the new transition model is performed for flows ranging from incompressible to hypersonic conditions.

15. SUBJECT TERMS
Turbulence; Transition; Boundary layer; Hypersonics

16. SECURITY CLASSIFICATION OF:			17. LIMITATION OF ABSTRACT	18. NUMBER OF PAGES	19a. NAME OF RESPONSIBLE PERSON STI Help Desk (email:help@sti.nasa.gov)
a. REPORT U	b. ABSTRACT U	c. THIS PAGE U	UU	35	19b. TELEPHONE NUMBER *(include area code)* 301-621-0390

Standard Form 298 (Rev. 8-98)
Prescribed by ANSI Std. Z39-18